Inorganica Chimica Acta 405 (2013) 24–30

Contents lists available at SciVerse ScienceDirect

Inorganica Chimica Acta

journal homepage: www.elsevier.com/locate/ica

Donation and scavenging of nitric oxide (NO) by flipping of the denticity of carboxylate ligand in novel ruthenium complexes: Photolability of the coordinated NO

Kaushik Ghosh *, Sushil Kumar, Rajan Kumar

Department of Chemistry, Indian Institute of Technology, Roorkee, Roorkee 247667, Uttarakhand, India

ARTICLE INFO

Article history:
Received 16 January 2013
Received in revised form 28 March 2013
Accepted 25 April 2013
Available online 3 May 2013

Keywords:
Ruthenium nitrosyl complex
Carboxylate ligand
Photolability
NO scavenging activity
Griess reaction
DPPH quenching study

ABSTRACT

Novel ruthenium nitrosyl complex $[Ru(\eta^1\text{-}L^1)(PPh_3)_2(NO)Cl_2]$ (**2**) (where L^1H is 3-chlorobenzoic acid and H is dissociable proton) was synthesized and characterized by spectroscopic and electrochemical studies. Molecular structure of complex **2** was determined by X-ray crystallography. The diamagnetic behaviour of **2** was established by NMR spectral studies and redox property of **2** was investigated. DFT optimization of the structure of **2** provided a linear geometry of $\{Ru^{II}\text{–}NO^+\}$ moiety. The nitrosyl complex acted as novel nitric oxide (NO) donor upon illumination of light and photoreleased NO was trapped by reduced myoglobin. Amount of photolytically cleaved NO was quantified by Griess reagent. The precursor complex $[Ru(\eta^2\text{-}L^1)(PPh_3)_2Cl_2]$ (**1**) was obtained after photorelease of NO and was found to be a potential NO scavenger. Flipping of denticity of carboxylate ligand was observed during NO donation and scavenging. DPPH (2,2-diphenyl-1-picrylhydrazine) radical quenching assay was performed to estimate the amount of generated reactive nitrogen species or/and reactive oxygen species during photolysis of NO.

1. Introduction

Carboxylates are an important class of organic oxo-anionic ligands which bind to metal ions in different coordination modes [1,2] and constitute a large variety of coordination complexes. In biosystem, amino acids having carboxylate function (e.g. aspartic acid and glutamic acid) in their side chains, are found in the metal-site(s) of several metalloproteins [2,3]. Hence, metal complexes ligated to carboxylato ligand are often used for the structural and functional modeling of metalloproteins [3,4]. Moreover binding of calcium and magnesium ions by carboxylate function is important for biological activities [3]. In recent past, considering the research in the field of inorganic chemistry, a remarkable example of versatile coordination chemistry exhibited by this oxo-anionic ligand, would be the synthesis of metalloorganic frameworks (MOFs). Systematic use of building blocks having carboxylate functional group(s) gave rise to a gamut of MOFs [5].

Research interest in the area of interaction of nitric oxide (NO) with transition metal complexes has grown extensively in the recent years [6,7]. Nitric oxide synthase (NOS) enzyme is responsible for the generation of NO in biosystem and NO is known to be involved in several biological pathways. It has been also found out that biological activities exhibited by NO are concentration dependent [7c]. Hence the molecules which could donate [6–10] as well as those compounds which could scavange [11] NO are extremely important for the treatment of diseases caused by unusual concentration of NO. There are several organic molecules which are used for NO delivery, however controlled and target specific delivery of NO could be achieved by inorganic complexes. For example, compounds which could deliver NO upon illumination of light are useful in photodynamic therapy (PDT) [7a,8c,12].

Investigation of literature revealed that in very few cases ruthenium complexes having carboxylate ligand(s) were used for the coordination and delivery of NO [7b,11]. During last few years, we have been working with ruthenium nitrosyl complexes which could deliver and/or scavenge NO [10]. Herein we report very simple but useful ruthenium complexes $[Ru(\eta^2\text{-}L^1)(PPh_3)_2Cl_2]$ (**1**) and $[Ru(\eta^1\text{-}L^1)(PPh_3)_2(NO)Cl_2]$ (**2**) (where L^1H = 3-chlorobenzoic acid and H is dissociable proton) (Scheme 1) for scavenging and donation of NO respectively. These complexes flip the denticity of carboxylato ligand during coordination and photolability of NO and to the best of our knowledge, there is no such report available in the literature. The molecular structure of the nitrosyl complex **2** was determined by X-ray crystallography.

The photodissociation of NO was examined under visible as well as in UV light. The amount of photoreleased NO was quantified using Griess reagent and the data was compared with the data obtained from sodium nitroprusside (SNP) under the same experimental conditions. Photoreleased NO obtained from **2** was trapped

* Corresponding author. Fax: +91 1332 273560.
E-mail address: ghoshfcy@iitr.ernet.in (K. Ghosh).

0020-1693/$ - see front matter © 2013 Elsevier B.V. All rights reserved.
http://dx.doi.org/10.1016/j.ica.2013.04.042

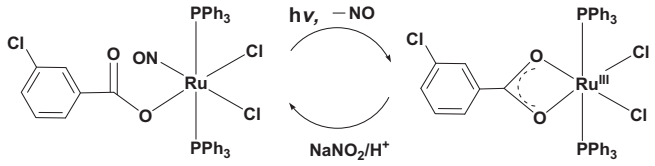

$[Ru(\eta^1\text{-}L^1)(PPh_3)_2(NO)Cl_2]$ (**2**) $[Ru(\eta^2\text{-}L^1)(PPh_3)_2Cl_2]$ (**1**)

Scheme 1. $\eta^1 \rightarrow \eta^2$ flipping of carboxylate group during photorelease and coordination of nitric oxide.

by reduced myoglobin and amount of the generated reactive nitrogen species and/or reactive oxygen species during photolysis reaction was determined by DPPH (2,2-diphenyl-1-picrylhydrazine) radical quenching studies. The NO scavenging activity of complex $[Ru(\eta^2\text{-}L^1)(PPh_3)_2Cl_2]$ (**1**) will also be scrutinized in this report.

2. Experimental

2.1. General procedures

All the chemicals used were of reagent grade. Analytical grade reagents sodium nitrite, 3-chloroperbenzoic acid (Sigma Aldrich, Steinheim, Germany), $RuCl_3{\cdot}3H_2O$, triphenylphosphine (SRL, Mumbai, India), naphthylethylenediamine dihydrochloride (NED), sulfanilamide (Himedia Laboratories Pvt., Ltd., Mumbai, India), disodium hydrogen phosphate anhydrous (RFCL Ltd., New Delhi, India) and sodium dihydrogen phosphate (Chemport India Pvt., Ltd. Mumbai, India) were used as obtained. Double distilled water was used in all the experiments. Equine skeletal muscle myoglobin was obtained from Sigma Aldrich, Steinheim, Germany.

^1H and ^{31}P NMR spectra were recorded on Bruker AVANCE, 500.13 MHz spectrometer in the deuterated solvents. Electronic absorption spectra of complexes **1** and **2** were recorded with Evolution 600, Thermo Scientific UV–Vis spectrophotometer. Infrared spectra were recorded on Thermo Nicolet Nexus FTIR spectrophotometer and were obtained in KBr pellets using 16 scans (in cm^{-1}). Cyclic voltammetric study was performed on a CH-600 electroanalyzer in dichloromethane solution with 0.1 M tetrabutylammonium perchlorate (TBAP) as supporting electrolyte. The working electrode, reference electrode and auxiliary electrode were glassy carbon electrode, Ag/AgCl electrode and Pt wire respectively. The concentration of the compound was $\sim 10^{-3}$ M. The ferrocene/ferrocenium couple appeared at $E_{1/2} = +0.52$ (92) V versus Ag/AgCl (scan rate 0.1 V/s) in dichloromethane under the same experimental conditions. Chemical actinometry study (with ferrioxalate actinometer) was performed to determine the quantum yield of photoreleased NO. The ESI-mass spectrum of the sample (methanolic solution was used) was recorded in the positive ion mode using Thermo Finnigan LCQ Deca mass spectrometer.

2.2. Synthesis of $[Ru^{III}(\eta^2\text{-}L^1)(PPh_3)_2Cl_2]$ (**1**)

Complex **1** was synthesized from the reaction of $Ru(PPh_3)_3Cl_2$ with 3-chloroperbenzoic acid (where L^1H = 3-chlorobenzoic acid and H is dissociable proton) in dichloromethane under nitrogen atmosphere according to the method reported earlier [13].

2.3. Synthesis of $[Ru(\eta^1\text{-}L^1)(PPh_3)_2(NO)Cl_2]$ (**2**)

A batch of complex **1** (0.043 g, 0.05 mmol) was dissolved in 25 mL of dichloromethane to obtain a red brown solution in round bottom flask of 100 mL. To the above solution, sodium nitrite (0.4 g, 6 mmol) with acidified distilled water (20 mL, pH 3.0) was added and the mixture was stirred at room temperature for an hour to get yellowish orange solution of complex **2**. Dichloromethane layer was separated out and the solvent was evaporated under dark conditions. Complex **2** (0.032 g, 0.036 mmol) was eluted from an alumina column by dichloromethane:methanol (9:1) mixture. To obtain single crystals of **2** for X-ray crystallography, a solution of **2** in dichloromethane/methanol mixture was kept in vapor diffusion of diethyl ether. Yield: 72%. *Anal.* Calc. for $C_{43}H_{34}NCl_3O_3P_2Ru$ (882.11): C, 58.55; H, 3.88; N, 1.59. Found: C, 58.49; H, 4.11; N, 1.61%. IR (KBr disk, cm^{-1}): 1880 (ν_{NO}), 1620(ν_{CO}), 1570, 1482, 1434, 1318, 1264, 1190, 1092, 745, 692, 518 (ν_{PPh3}) cm^{-1}. UV–Vis (CH_2Cl_2; λ_{max}, nm (ε, $M^{-1}\,cm^{-1}$)): 237 (35 084), 320 (27 017). ^{31}P NMR ($CDCl_3$, 500 MHz): δ 16.55 ppm. ^1H NMR ($CDCl_3$, 500 MHz): δ 7.85–7.81 (m, 12H), 7.35–7.28 (m, 18H), 7.24 (s, 1H), 7.21 (d, 1H), 7.18 (d, 1H), 7.00 (t, 1H).

2.4. Griess reagent assay

Griess reagent was prepared by mixing equal volumes of 1% sulphanilamide in 5% orthophosphoric acid and 0.1% naphthylethylenediamine dihydrochloride (NED) in distilled water. The estimation of NO or nitrite (NO_2^-) ion was measured by observing the increase in the absorbance near 538 nm due to the formation of azo dye. Aqueous solutions of sodium nitrite with different concentrations (5–50 μM) were used to prepare standard curve for the determination of nitrite [10a].

2.5. Quantum yield measurements

Standard ferrioxalate actinometer (0.006 M solution of potassium ferrioxalate in 0.1 N H_2SO_4) was used to determine the intensity of the UV light (λ_{irr} = 365 nm). Quantum yield (Φ_{NO}) of NO photorelease for complex **2** was determined from the decrease in its absorption band with λ_{max} near 320 nm when irradiated with the light of a UV lamp (λ_{irr} = 365 nm) and was calculated by following the procedure reported earlier [10a]. The cuvette was kept 3 cm away from the UV source to measure the quantum yields.

2.6. DFT study and computational details

The DFT calculation for complex **2** was carried out using GAUSSIAN *03* program package [14,15]. The Becke's three parameters hybrid exchange functional with the Lee–Yang–Parr (LYP) non-local correlation functional was used throughout the computational study [9a,15,16]. A LANL2DZ basis set [14] for ruthenium metal and 6-31G(d) basis set [9a,14a] for non metal atoms was used in the calculation. The coordinates oobtained from X-ray crystal structure were used as input data for geometry optimization. The Gauss View-4 program was used for pictorial representation of spin densities and frontier molecular orbitals. The NO stretching frequency was calculated using scaling factor of 0.97 for LANL2DZ basis set [17].

2.7. X-ray crystallography

Red orange crystals of complex **2**, suitable for diffraction study, were obtained *via* vapor diffusion of diethyl ether into a solution of **2** in dichloromethane/methanol mixture. The X-ray data collection and processing for complex **2** was performed on Bruker Kappa Apex–II CCD diffractometer by using graphite monochromated Mo Kα radiation (λ = 0.71073 Å) at 273 K. Crystal structure was solved by direct method. All calculations were performed using the SHELXTL [18,19] software package for structure solution and refinement. All non-hydrogen atoms were refined anisotropically. Hydrogen atoms were placed in geometrically calculated positions

and refined using a riding model. The images were created with the DIAMOND program [20].

2.8. DPPH quenching assay

Amount of NO as well as other reactive oxygen and/or reactive nitrogen species was estimated by DPPH radical quenching assay using UV–Vis spectrophotometer [21]. The electronic spectra were recorded in dichloromethane solutions. UV–Vis spectrum of DPPH radical ($\sim 3.5 \times 10^{-5}$ M) showed a band near 520 nm. Now a dichloromethane solution of **2** ($\sim 5.0 \times 10^{-5}$ M) was added to the same solution. There was no loss of NO when the solution mixture was kept in dark for 30 min. Exposure of low intensity UV light to the same solution resulted in the disappearance of the band near 520 nm (electronic spectra were recorded at 30 s intervals). The decrease in electronic absorption spectrum of DPPH radical in presence of **2** clearly depicted the formation NO and/or any other radical species in solution.

2.9. Preparation of phosphate buffer and myoglobin (Mb) stock solution

A 50 mM phosphate buffer solution of pH 6.8 was prepared by adding 0.4192 g of $NaH_2PO_4{\cdot}2H_2O$ and 0.3283 g of anhydrous Na_2HPO_4 to 50 mL of MilliQ water. The volume of the solution was made 100 mL in volumetric flask. Now to prepare myoglobin stock solution, 5 mg of equine skeletal muscle myoglobin was dissolved in 5 mL of buffer solution (vide infra). 100 μL of myoglobin stock solution was diluted to 1 mL in a quartz cuvette with an optical length of 1 cm and was sealed with a rubber septum.

3. Results and discussion

3.1. Syntheses

A brown red complex $[Ru^{III}(\eta^2\text{-}L^1)(PPh_3)_2Cl_2]$ (**1**) (where L^1H = 3-chlorobenzoic acid and H is dissociable proton) was synthesized from the reaction of $Ru(PPh_3)_3Cl_2$ with 3-chloroperbenzoic acid under nitrogen atmosphere [13]. A dichloromethane solution of **1** was treated with *in situ* generated NO derived from acidified sodium nitrite solution (pH 3.0) to obtain the nitrosyl complex $[Ru(\eta^1\text{-}L^1)(PPh_3)_2(NO)Cl_2]$ (**2**) (Scheme 1) in good yield. Both the complexes (**1** and **2**) were found to be highly soluble in all the organic solvents such as dichloromethane, benzene, methanol, acetonitrile and dimethylformamide, however they were less soluble in water. Complex **2** was recrystallized from the vapor diffusion of diethyl ether into dichloromethane/methanol solution.

3.2. General properties

Complex **2** was obtained by the reaction of non-innocent ligand NO with complex **1** and $\{RuNO\}^6$ moiety was found to be present in **2** [22]. The NO stretching frequency (ν_{NO}) appeared at 1880 cm^{-1} in the IR spectrum of complex **2** (shown in Fig. S1). This was expected for ruthenium nitrosyl complexes having $\{Ru\text{–}NO\}^6$ moiety [7b]. The value of ν_{NO} was in the range of 1820–1960 cm^{-1} and a description of $\{Ru^{II}\text{–}NO^+\}^6$ was proposed for $\{Ru\text{–}NO\}^6$ species [7b]. The appearance of a peak at $\sim$1625 cm^{-1} in the IR spectrum of **2** supported the presence of metal ligated monodentate carboxylate group [23]. The presence of phosphine ligands was clearly indicated by IR bands near 750, 692 and 518 cm^{-1} for both the complexes [10].

The electronic absorption spectra of complexes **1** and **2** are displayed in Fig. S2. UV–Vis spectrum of complex **1** exhibited two absorbtion bands near 283 nm and 296 nm. On the other hand, absorption spectrum of **2** afforded a metal to ligand charge transfer (MLCT) transition near 320 nm. It is well known in the literature that the photolability of NO arises by photo-excitation of electron from $d\pi(M) \rightarrow \pi^*(NO)$ in nitrosyl complexes [7a,7b]. Hence, these bands are important for the application of nitrosyl complexes in photodynamic therapy PDT [7a].

Complex **2** was found to be diamagnetic which was confirmed by ^1H and ^{31}P NMR spectral studies (Figs. S3 and S4). ^1H NMR spectrum of **2** showed expected multiple signals in the range of 6.5–8.0 ppm. A single resonance for two PPh_3 groups was found in the ^{31}P NMR spectrum of **2** at $\sim$16.55 ppm which authenticated the *trans* disposition of phosphine groups in complex **2** [10].

ESI-MS study for **2** was investigated in methanolic solution and experimental data was deposited in Fig. S5. The molecular ion peak at m/z = 881.01 $(M)^+$ for **2** was not detected in the ESI-mass spectrum, however the most abundant peak was observed at m/z = 727.8 $[M\text{-}(3\text{-chlorobenzoate})]^+$.

3.3. Description of molecular structure

Molecular structure of the complex $[Ru(\eta^1\text{-}L^1)(PPh_3)_2(NO)Cl_2]$ (**2**) is depicted in Fig. 1. The matrix parameters of this complex are described in Table 1 and the selected bond distances and bond angles are listed in Table 2. In the molecular structure of **2**, ruthenium center was found to be octahedrally coordinated having phosphine groups at the axial positions *trans* to each other. Nitrogen atom N1 from NO moiety, one carboxylato oxygen (O2) and two chlorine atoms (Cl1 and Cl2) constituted the equatorial plane. One chlorine atom (Cl1) was found at the position *trans* to NO. The Ru–N(NO) (1.704(8) Å) and N–O (N1–O1 = 1.164(7) Å) distances were consistent to the values reported in the literature [7,9]. The geometry was found to be distorted octahedral which was also reflected in all the bond parameters around ruthenium center in complex **2** (see Table 2).

Interestingly we have found that in precursor complex (**1**), carboxylate group was bidentate [13], however, after nitrosylation, one oxygen atom of –COO group was detached from the metal center and carboxylate group became monodentate. In precursor complex, the bidentate carboxylate ligand provided similar C–O bond distances [13], on the other hand in complex **2**, C1–O2 and C1–O3 bond distances were found to be 1.285(9) and 1.189(9) respectively. These data clearly indicated the monodentate behaviour of the carboxylato function and were similar to the values reported by Carmona et al. [24]. Ru–N and N–O distances along with

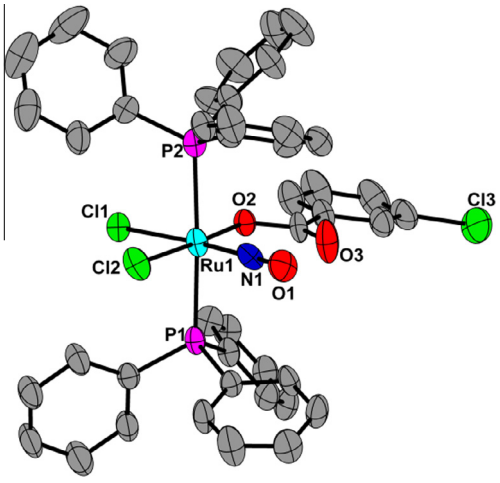

Fig. 1. ORTEP diagram (50% probability level) of the complex $[Ru(\eta^1\text{-}L^1)(PPh_3)_2(NO)Cl_2]$ (**2**). Hydrogen atoms are not shown for clarity.

Table 1
Crystal data and the structural refinement parameters for complex **2**.

Empirical formula	$C_{43}H_{34}Cl_3NO_3P_2Ru$
Formula weight	881.06
T (K)	273(2)
λ (Å) (Mo-Kα)	0.71073
Crystal system	monoclinic
Space group	$P21/n$
a (Å)	10.6581(14)
b (Å)	28.646(4)
c (Å)	14.0087(19)
α (°)	90.00
γ (°)	90.00
β (°)	109.646(9)
V (Å^3)	4028.0(10)
Z	4
ρ_{calc} (g cm^{-3})	1.453
F (000)	1792.0
θ (°)	1.42–27.50
Index ranges	$-13 < h < 13$, $-37 < k < 36$, $-18 < l < 18$
Data/restraints/parameters	9246/149/478
Goodness-of-fit[a] on F^2	1.362
R_1[b] [$I > 2\sigma(I)$]	0.1141
R_1 [all data]	0.2885
$wR2$[c] [$I > 2\sigma(I)$]	0.1416
$wR2$ [all data]	0.1718

[a] $GOF = [\Sigma[w(F_o^2 - F_c^2)^2]/M - N]^{1/2}$ (M = number of reflections, N = number of parameters refined).
[b] $R_1 = \Sigma||F_o| - |F_c||/\Sigma|F_o|$.
[c] $wR_2 = [\Sigma[w(F_o^2 - F_c^2)^2]/\Sigma[(F_o^2)^2]]^{1/2}$.

Ru–N–O angle (~173°) clearly expressed $\{Ru^{II}–NO^+\}^6$ description of diamagnetic $\{Ru–NO\}^6$ moiety [7b,22] This was also supported by IR and NMR spectral data and the presence of phosphine groups was also confirmed by ^{31}P NMR data in complex **2** (vide supra).

The non-covalent interactions have been found to be very much important for supramolecular chemistry and in engineering of crystals [25]. The intermolecular hydrogen bonding interactions found in the packing diagram of complex **2** are described in Table S1 and the interactions are shown in Fig. S6.

3.4. Theoretical calculations

Density functional theory (DFT) computations were employed to optimize the geometry of complex **2**. The calculation was carried out at B3LYP level [9a,14,16] of theory using LANL2DZ [14] basis set for ruthenium metal atom and 6-31G(d) basis set [14a] for non metal atoms (C, H, N, O, P and Cl). Effective core potential was employed in geometry optimization. The data obtained by geometry optimization of complex **2** was compared with the data afforded by X-ray crystallography. This comparison clearly indicated that the bond distances and angles in complex $[Ru(\eta^1\text{-}L^1)(PPh_3)_2(NO)Cl_2]$ (**2**) were reproduced quite well (shown in Table 2). In general, the computed bond lengths and bond angles are slightly deviated because the calculations are performed on complexes in gas phase. The computed ν(NO) harmonic vibrational frequency was found at ~1881 cm^{-1} (scaling factor was 0.97 for LANL2DZ basis set) [17]. The DFT optimized structure of **2** exhibited nearly linear geometry of $\{Ru^{II}–NO^+\}$ group in complex **2** with Ru–N–O angle of nearly 169°. The N–O bond distance (~1.15 Å) and N–O stretching frequency (ν_{NO}) at ~1881 cm^{-1} also supported the presence of $\{Ru^{II}–NO^+\}^6$ species in the optimized structure of complex **2**. It is important to note here that the $\{RuNO\}^6$ moiety present in **2** can be described either as a diamagnetic $\{Ru^{II}–NO^+\}$ species involving coordination of NO^+ to a low spin d^6 Ru^{II} center or as a diamagnetic $\{Ru^{III}–NO^{\cdot}\}$ species having coordination of a neutral $NO^{\cdot}$ to a low spin d^5 Ru^{III} center. In the nitrosyl complex containing $\{Ru^{II}–NO^+\}$ species, the Ru–N–O angle should be linear while in the diamagnetic $\{Ru^{III}–NO^{\cdot}\}$ species, the Ru–N–O angle should be bent. The value of Ru–N–O angle in the computed geometry clearly indicated the coordination of NO^+ to a low spin d^6 ruthenium(II) center. The major part of HOMO was found to be located over the metal center and the frontier molecular orbitals are shown in Fig. S7.

Table 2
Selected bond distances (Å) and bond angles (°) for complex **2** along with the optimized DFT bond parameters for comparison.

Bond distances (Å)			Bond angles (°)		
	X-ray	DFT		X-ray	DFT
Ru(1)–Cl(1)	2.356(2)	2.417	N(1)–Ru(1)–O(2)	98.8(3)	97.69
Ru(1)–Cl(2)	2.397(2)	2.487	Cl(1)–Ru(1)–Cl(2)	90.87(8)	92.12
Ru(1)–O(2)	2.077(5)	2.085	N(1)–Ru(1)–P(1)	90.1(2)	93.37
Ru(1)–N(1)	1.704(8)	1.770	O(1)–N(1)–Ru(1)	173.1(7)	168.76
Ru(1)–P(1)	2.440(2)	2.511	N(1)–Ru(1)–Cl(1)	175.3(2)	175.38
Ru(1)–P(2)	2.449(3)	2.513	P(1)–Ru(1)–P(2)	176.51(2)	172.54
N(1)–O(1)	1.164(7)	1.146	O(2)–Ru(1)–Cl(2)	176.44(17)	179.05
O(3)–C(1)	1.189(9)	1.241			
O(2)–C(1)	1.285(9)	1.300			

3.5. Electrochemistry

Cyclic voltammetric study was performed to examine the redox properties of ruthenium center in complex **2** in dichloromethane solution using 0.1 M tetrabutylammonium perchlorate (TBAP) as supporting electrolyte. In the precursor complex Ru^{III}/Ru^{II} was found near −0.4 V versus SCE [13]. On the other hand, only an irreversible cathodic peak near −0.87 V versus Ag/AgCl was observed for **2** (shown in Fig. S8). In the negative potential quasireversible couples (Ru^{III}/Ru^{II}) for nitrosyl complexes were reported [26] by Mascharak and coworkers. However, Lahiri and coworkers described ligand (nitric oxide) centered reduction $(Ru^{II}–NO^+) \rightarrow (Ru^{II}–NO^{\bullet})$ for the appearance of such peak [9b]. The appearance of irreversible cathodic peak clearly expressed that NO-centered reduction to afford a complex having $\{RuNO\}^7$ species is unfavorable.

3.6. Photolysis experiment for nitrosyl complex

The photolysis experiment of ~10^{-5} M solution of complex **2** in dichloromethane was carried out under visible light using 100 W

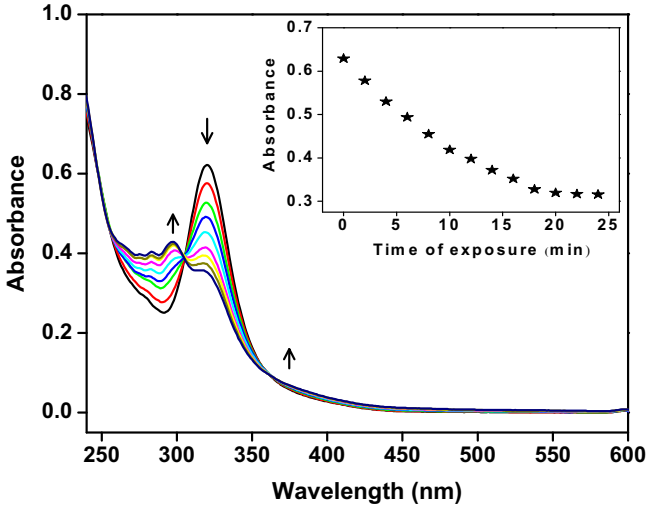

Fig. 2. Photodissociation of NO from **2** (~2.3×10^{-5} M) in dichloromethane under illumination of visible light (100 W tungsten lamp). Inset: Time dependent changes in absorbance with λ_{max} near 320 nm at room temperature.

tungsten lamp and light from an UV lamp (λ_{max} = 365 nm). Upon exposure to visible light, complex **2** afforded slow release of NO in dichloromethane solution (Fig. 2), however, a rapid spectral changes were observed when the same solution was exposed to low intensity light of UV lamp (shown in Fig. S9). During photolysis (in presence of visible as well as UV light), the electronic spectra of **2** showed the disappearance of the peak near 320 nm. Formation of new absorption peaks near 283 and 296 nm with two clear isosbestic points indicated photocleavage of NO upon illumination of light. A significant colour change from yellow to brown red was also observed after the photolysis experiment. Interestingly, we observed that the electronic spectrum of the photoproduct of complex **2** was similar to the absorption spectrum of complex **1**. This data prompted us to characterize the resultant complex after photolysis experiment.

In our previous report, we have investigated the reversible binding of phenolato oxygen with the coordination and photolability of NO and the photoproduct was having metal in 3+ oxidation state [10b]. Herein, the reversible binding of carboxylato-O function was found during the photodissociation and coordination of NO (Scheme 1). The photocleavage of NO was also examined using FTIR spectral study in solution. We observed reduced intensities at 1880 and 1625 cm^{-1} of the nitrosyl and carbonyl bands respectively after visible light (100 Watt W-lamp) illumination (shown in Fig. 3).

3.7. Griess reagent assay: quantification of photoreleased NO

By using Griess reagent assay [10a], we have estimated the amount of photoreleased NO from complex **2** upon illumination of UV and visible light. In this reaction, a negligible amount of NO was found to be released in dark, however, an increase in the intensity of the band near 538 nm under UV as well as visible light (Fig. 4 and Fig. S12) clearly indicated the photorelease of NO and concomitant formation of azo dye. Sodium nitroprusside (SNP) is known to be a standard drug for delivery of nitric oxide [7b,7d]. A simultaneous measurement of NO release from SNP was also investigated for the comparison of our data. In Griess reaction, exposure of UV light for 15 min to 50 μM solution of the complex **2** gave rise to 18 to 20 μM of available NO (Fig. 4). However, in case of SNP (50 μM), the amount was found to be ~4 μM of NO (Fig. 5(a)). In visible light, the NO production by complex **2** was very slow and the amount was around 8 μM (same exposure time, Fig. 5(b)). This data clearly indicated the photorelease of NO in solution and the concentration of free NO in complex **2** was found to be more as compared to NO released by sodium nitroprusside.

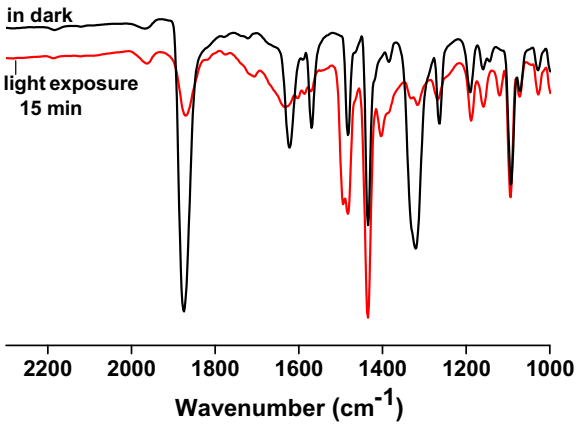

Fig. 3. Infrared spectra showing photorelease of NO from **2** with the exposure of visible light for 10–15 min.

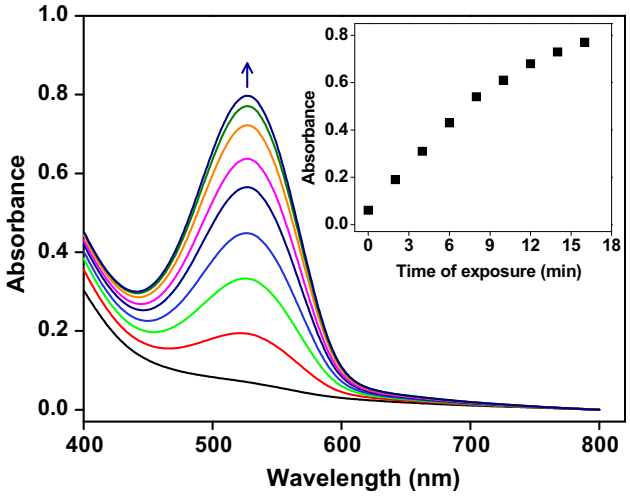

Fig. 4. Electronic spectra of the formation of dye when Griess reagent (100 μL) was treated with complex **2** (50 μM) in the presence of light of UV lamp (λ_{max} = 365 nm). Inset: Time dependent changes in absorbance at λ = 538 nm at room temperature.

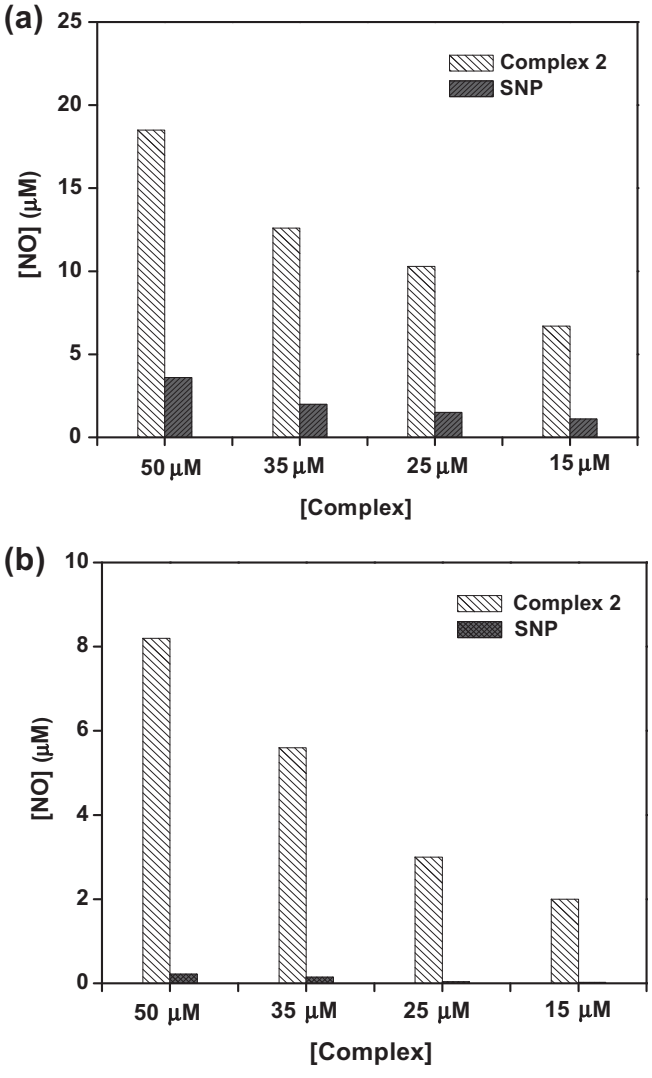

Fig. 5. Bar diagrams to compare the amount of photoreleased NO (dye formation) from the complex **2** with sodium nitroprusside (SNP) under exposure of (a) UV light and (b) visible light for 15 min.

The quantum yield (ϕ) for NO photorelease from complex **2** (λ_{irr} = 365 nm) was found to be 0.018 ± 0.001 in dichloromethane solution [10a] Fig. 5.

3.8. Scavenging of NO by complex $[Ru^{III}(\eta^2\text{-}L^1)(PPh_3)_2Cl_2]$ (**1**)

We have observed that the photoproduct of complex **2** was complex **1**. This prompted us to study complex **1** as NO scavenger by using UV–Vis spectroscopy. Electronic absorption spectra were taken in absence and in presence of complex **1**. Nitric oxide scavenging ability of complex **1** was observed by Griess reagent assay with sodium nitrite. The production of nearly 24 μM of NO was detected when 25 μM aqueous solution of sodium nitrite was prepared in a 1 mL cuvette with 100 μL of the Griess reagent (see Fig. S11). The presence of 50 μM concentration of complex **1** in the same cuvette lowers the concentration of produced NO from 24 to 4 μM (shown in Fig. 6). These data explain that **1** exhibits high affinity for NO and could scavenge nitric oxide.

3.9. NO trapping by reduced myoglobin

The photoreleased NO from complex **2** was trapped by reduced myoglobin (Mb) (Fig. S14). The electronic absorption spectrum for oxidized myoglobin (Mb) (concentration ~2.8×10^{-6} M) showed an intense band with λ_{max} near 409 nm (Soret band). The UV–Vis spectrum of reduced myoglobin near 433 nm was obtained by addition of excess sodium dithionite. No reaction was observed, when acetonitrile solution of complex **2** (~7.5×10^{-5} M) was added to buffer solution of reduced myoglobin under dark conditions. The same solution mixture was kept under exposure to the light of UV lamp (λ_{max} = 365 nm) for 60 s and absorption spectrum of the solution afforded a peak near 420 nm indicating the formation of Mb–NO adduct [10,26a].

3.10. DPPH radical quenching studies

DPPH (2,2-diphenyl-1-picrylhydrazine) is an intensely violet-colored stable free radical which is used to determine the antioxidant properties of different amines, phenols, natural products, foods etc. [21]. DPPH radical has been used as free radical

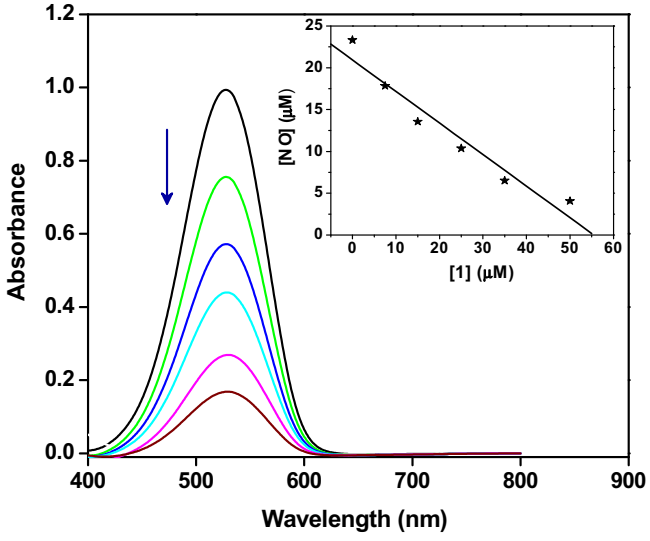

Fig. 6. Electronic spectra showing scavenging of NO in the presence of different concentrations (7.5–50 μM) of complex **1** in Griess assay (Griess reagent and sodium nitrite). Inset: Change in amount of dye formation with different concentrations of **1** with Griess assay.

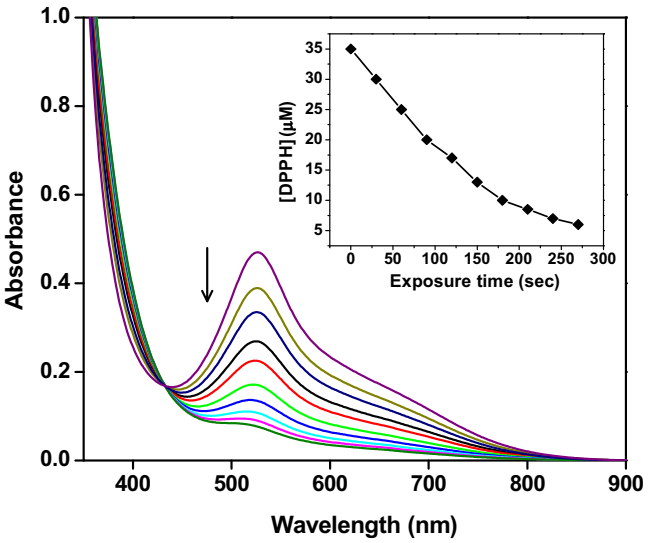

Fig. 7. Reaction of photocleaved NO from **2** (~5.0×10^{-5} M) with DPPH radical (~3.5×10^{-5} M) in dichloromethane solution. Inset: Time dependent changes in absorbance of DPPH radical at λ_{max} near 520 nm at room temperature.

scavenger [21a] and it participates in homolytic additions with other radical species. The reactions of DPPH with different reactive oxygen and reactive nitrogen species have been widely studied where violet colour of DPPH turns to light yellow colour (with a λ-shift from 520 to 320 nm) and the antioxidant properties are quantified. We were interested to observe the disappearance of intense violet colour in presence of NO from the nitrosyl complex **2**, keeping in mind that NO itself as well as other reactive species could decolorise the solution of DPPH radical. A dichloromethane solution of **2** (~10^{-5} M) was exposed to light in presence of the DPPH radical (~3.5×10^{-5} M) and we observed a decrease in absorbance of DPPH near 520 nm (shown in Fig. 7).

We estimated the amount of reactive oxygen and/or reactive nitrogen species generated due to photorelease of free NO radical from **2** by monitoring the decrease in absorbance of DPPH (~35 μM) near 520 nm. Amount of reactive species was found nearly 30 μM when the solution was exposed to UV light for 5 min.

4. Conclusions

Following are the important findings of the present report. First, we have synthesized and characterized a simple but novel ruthenium nitrosyl complex which is useful for controlled NO delivery. The ruthenium nitrosyl complex was photolabile and this complex demands its possible applications in photodynamic therapy (PDT). Second, the photoliberated NO was tranferred to reduced myoglobin and concentration of available NO was determined by using Griess reagent assay. Third, generation of reactive oxygen species and/or reactive nitrogen species during NO photolysis was investigated by DPPH radical quenching assay. Forth, interestingly, the precursor ruthenium complex (**1**) was obtained after NO delivery. Hence, a unique flipping of $\eta^1 \rightarrow \eta^2$ denticity of carboxylate function was observed during NO coordination and delivery. Fifth, the precursor complex (**1**) was found an excellent candidate for NO scavenging activity. Hence, attachment of $[Ru(PPh_3)_2(Cl)_2(NO)]$ moiety with biomolecules having –COOH function could be explored. We would like to mention here that the reaction of $[Ru^{III}(PPh_3)_2(Cl)_3(MeOH)]$ [27] and benzoic acid also afforded complex similar to complex **1**. Most important is the simplicity of this system as –COOH group is present in several molecules namely

Scheme and Table captions

non-steroidal anti-inflammatory drugs (NSAIDs) and protein side-chains etc. Water solubility could easily be changed by using different phosphines [28]. Synthesis of other related complexes for delivery and their biological applications are under progress.

Acknowledgements

K. G is thankful to CSIR, India for financial assistance (01(2229)/08/EMR-II dated 06-MAR-2008). S. K and R. K are thankful to CSIR for financial support. We are also thankful for FIG-Scheme-B funded by IIT Roorkee.

Appendix A. Supplementary material

Characterization of complexes by IR and NMR spectral studies. The standard curve of $NaNO_2$ for Griess reaction. The trapping of nitric oxide by myoglobin and X-ray crystallographic data of complex in CIF format. Supplementary data associated with this article can be found, in the online version, at http://dx.doi.org/10.1016/j.ica.2013.04.042.

References

[1] F.A. Cotton, G. Wilkinson, C.A. Murillo, M. Bochmann, Advanced Inorganic Chemistry, sixth ed., John Wiley and Sons, New York, USA, 1999, p. 486.
[2] (a) S.J. Lippard, J.M. Berg, Principles of Bioinorganic Chemistry, University Science Books, Panima Publishing Corp., New Delhi, India, 2005, p. 260.;
(b) W. Kaim, B. Schwederski, Bioinorganic Chemistry: Inorganic Elements in the Chemistry of Life, John Wiley and Sons, Chichester, England, 2001.
[3] (a) T. Dudev, C. Lim, Acc. Chem. Res. 40 (2007) 85;
(b) Z. Xia, D.R. Storm, Nat. Rev. Neurosci. 6 (2005) 267.
[4] (a) E.Y. Tshuva, S.J. Lippard, Chem. Rev. 104 (2004) 987;
(b) M. Costas, C.W. Cady, S.V. Kryatov, M. Ray, M.J. Ryan, E.V. Rybak-Akimova, L. Que Jr., Inorg. Chem. 42 (2003) 7519;
(c) L.H. Do, T. Hayashi, P. Moenne-Loccoz, S.J. Lippard, J. Am. Chem. Soc. 132 (2010) 1273.
[5] (a) H. Furukawa, N. Ko, Y.B. Go, N. Aratani, S.B. Choi, E. Choi, A.O. Yazaydin, R.Q. Snurr, M. O'Keeffe, J. Kim, O.M. Yaghi, Science 329 (2010) 424;
(b) J.R. Long, O.M. Yaghi, Chem. Soc. Rev. 38 (2009) 1213.
[6] (a) W. Kaim, B. Schwederski, Coord. Chem. Rev. 254 (2010) 1580;
(b) F. Roncaroli, M. Videla, L.D. Slep, J.A. Olabe, Coord. Chem. Rev. 251 (2007) 1903;
(c) J. Heinecke, P.C. Ford, Coord. Chem. Rev. 254 (2010) 235;
(d) G.B. Richter-Addo, P. Legzdins, J. Burstyn, Chem. Rev. 102 (2002) 857;
(e) P.C. Ford, L.E. Laverman, Coord. Chem. Rev. 249 (2005) 391;
(f) T.W. Hayton, P. Legzdins, W.B. Sharp, Chem. Rev. 102 (2002) 935;
(g) T.C. Berto, A.L. Speelman, S. Zheng, N. Lehnert, Coord. Chem. Rev. 257 (2013) 244;
(h) N. Xu, J. Lilly, D.R. Powell, G.B. Richter-Addo, Organometallics 31 (2012) 827.
[7] (a) N.L. Fry, P.K. Mascharak, Acc. Chem. Res. 44 (2011) 289;
(b) M.J. Rose, P.K. Mascharak, Coord. Chem. Rev. 252 (2008) 2093;
(c) M.J. Rose, P.K. Mascharak, Curr. Opin. Chem. Biol. 12 (2008) 238;
(d) A.A. Eroy-Reveles, Y. Leung, C.M. Beavers, M.M. Olmstead, P.K. Mascharak, J. Am. Chem. Soc. 130 (2008) 4447;
(e) M.J. Rose, P.K. Mascharak, Chem. Commun. (2008) 3933.
[8] (a) P.C. Ford, Inorg. Chem. 49 (2010) 6226;
(b) A.D. Ostrowski, P.C. Ford, Dalton Trans. (2009) 10660;
(c) P.C. Ford, Acc. Chem. Res. 41 (2008) 190;
(d) M.G. Sauaia, R.G. de Lima, A.C. Tedesco, R.S. da Silva, Inorg. Chem. 44 (2005) 9946;
(e) M.G. Sauaia, R.G. de Lima, A.C. Tedesco, R.S. da Silva, J. Am. Chem. Soc. 125 (2003) 14718.
[9] (a) P. De, S. Maji, A.D. Chowdhury, S.M. Mobin, T.K. Mondal, A. Paretzki, G.K. Lahiri, Dalton Trans. 40 (2011) 12527;
(b) N. Chanda, D. Paul, S. Kar, S.M. Mobin, A. Datta, V.G. Puranik, K.K. Rao, G.K. Lahiri, Inorg. Chem. 44 (2005) 3499.
[10] (a) K. Ghosh, S. Kumar, R. Kumar, U.P. Singh, Eur. J. Inorg. Chem. (2012) 929;
(b) K. Ghosh, S. Kumar, R. Kumar, U.P. Singh, N. Goel, Organometallics 30 (2011) 2498;
(c) K. Ghosh, S. Kumar, R. Kumar, U.P. Singh, N. Goel, Inorg. Chem. 49 (2010) 7235.
[11] (a) B.R. Cameron, M.C. Darkes, H. Yee, M. Olsen, S.P. Fricker, R.T. Skerlj, G.J. Bridger, N.A. Davies, M.T. Wilson, D.J. Rose, J. Zubieta, Inorg. Chem. 42 (2003) 1868;
(b) B.R. Cameron, M.C. Darkes, I.R. Baird, R.T. Skerlj, Z.L. Suntucci, S.P. Fricker, Inorg. Chem. 42 (2003) 4102;
(c) S.P. Fricker, Platinum Met. Rev. 39 (1995) 150.
[12] A.K. Patra, R. Afshar, M.M. Olmstead, P.K. Mascharak, Angew. Chem., Int. Ed. 41 (2002) 2512 (and references therein).
[13] S. Chattopadhyay, N. Bag, P. Basu, G.K. Lahiri, A. Chakravorty, J. Chem. Soc., Dalton Trans. (1990) 3389.
[14] (a) K. Karidi, A. Garoufis, A. Tsipis, N. Hadjiliadis, H. den Dulk, J. Reedijk, Dalton Trans. (2005) 1176;
(b) M. Videla, J.S. Jacinto, R. Baggio, M.T. Garland, P. Singh, W. Kaim, L.D. Slep, J.A. Olabe, Inorg. Chem. 45 (2006) 8608.
[15] M.J. Frisch, G.W. Trucks, H.B. Schlegel, G.E. Scuseria, M.A. Robb, J.R. Cheeseman, J.A. Jr. Montgomery, T. Vreven, K.N. Kudin, J.C. Burant, J.M. Millam, S.S. Iyengar, J. Tomasi, V. Barone, B. Mennucci, M. Cossi, G. Scalmani, N. Rega, G.A. Petersson, H. Nakatsuji, M. Hada, M. Ehara, K. Toyota, R. Fukuda, J. Hasegawa, M. Ishida, T. Nakajima, Y. Honda, O. Kitao, H. Nakai, M. Klene, X. Li, J.E. Knox, H.P. Hratchian, J.B. Cross, C. Adamo, J. Jaramillo, R. Gomperts, R.E. Stratmann, O. Yazyev, A.J. Austin, R. Cammi, C. Pomelli, J.W. Ochterski, P.Y. Ayala, K. Morokuma, G.A. Voth, P. Salvador, J.J. Dannenberg, V.G. Zakrzewski, S. Dapprich, A.D. Daniels, M.C. Strain, O. Farkas, D.K. Malick, A.D. Rabuck, K. Raghavachari, J.B. Foresman, J.V. Ortiz, Q. Cui, A.G. Baboul, S. Clifford, J. Cioslowski, B.B. Stefanov, G. Liu, A. Liashenko, P. Piskorz, I. Komaromi, R.L. Martin, D.J. Fox, T. Keith, M.A. Al-Laham, C.Y. Peng, A. Nanayakkara, M. Challacombe, P.M.W. Gill, B. Johnson, W. Chen, M.W. Wong, C. Gonzalez, J.A. Pople, GAUSSIAN 03 revision E.01, Gaussian Inc., Pittsburgh, PA, 2007.
[16] (a) A.D. Becke, J. Chem. Phys. 96 (1992) 2155;
(b) A.D. Becke, J. Chem. Phys. 98 (1993) 5648.
[17] M. Pagliai, L. Bellucci, M. Muniz-Miranda, G. Cardini, V. Schettino, Phys. Chem. Chem. Phys. 8 (2006) 171.
[18] G.M. Sheldrick, Acta. Crystallogr., Sect. A 46 (1990) 467.
[19] G.M. Sheldrick, SHELXTL–NT 2000 version 6.12, Reference Manual, University of Gottingen, Pergamon, New York, 1980.
[20] B. Klaus, University of Bonn, Germany DIAMOND, Version 1.2 c, 1999.
[21] (a) P. Ionita, Chem. Pap. 59 (2005) 11;
(b) H.-M. Kang, M.E. Saltveit, J. Agric. Food Chem. 50 (2002) 513;
(c) A. Chandrasekara, F. Shahidi, J. Agric. Food Chem. 59 (2011) 428;
(d) M.C. Foti, C. Daquino, C. Geraci, J. Org. Chem. 69 (2004) 2309;
(e) H. Aoshima, H. Tsunoue, H. Koda, Y. Kiso, J. Agric. Food Chem. 52 (2004) 5240.
[22] J.H. Enemark, R.D. Feltham, Coord. Chem. Rev. 13 (1974) 339.
[23] (a) K. Majumder, S. Bhattacharya, Polyhedron 18 (1999) 3669;
(b) V. Djinovic, M. Momcilovic, S. Grguric-Sipka, V. Trajkovic, M.M. Stojkovic, D. Miljkovic, T. Sabo, J. Inorg. Biochem. 98 (2004) 2168.
[24] D. Carmona, F. Viguri, M.P. Lamata, J. Ferrer, E. Bardaji, F.J. Lahoz, P. Garcia-Orduna, L.A. Oro, Dalton Trans. 41 (2012) 10298.
[25] G.R. Desiraju, T. Steiner, The Weak Hydrogen Bond in Structural Chemistry and Biology, Oxford University Press, New York, 1999.
[26] (a) A.K. Patra, P.K. Mascharak, Inorg. Chem. 42 (2003) 7363;
(b) M.J. Rose, A.K. Patra, E.A. Alcid, M.M. Olmstead, P.K. Mascharak, Inorg. Chem. 46 (2007) 2328.
[27] T.A. Stephenson, G. Wilkinson, J. Inorg. Nucl. Chem. 28 (1966) 945.
[28] A. Katho, Z. Opre, G. Laurenczy, F. Joo, J. Mol. Catal. A: Chem. 204–205 (2003) 143.